

Supporting Information

Self-Assembly of Thiolate-Protected Silver Coordination Polymers Regulated by POMs

Ya-Hui Li,^a Zhao-Yang Wang,^a Bing Ma,^b Hong Xu,^{*a} Shuang-Quan Zang^{*a} and Thomas C. W. Mak^c

^a *Green Catalysis Center, and College of Chemistry, Zhengzhou University, Zhengzhou, Henan 450001, P. R. China.*

^b *Université de Paris, Laboratoire d'Electrochimie Moléculaire, CNRS, Paris, France*

^c *Department of Chemistry and Center of Novel Functional Molecules, The Chinese University of Hong Kong, Shatin, New Territories, Hong Kong, China.*

*E-mail: zangsqzg@zzu.edu.cn

xuhong@zzu.edu.cn

Materials and reagents

AgS^tBu, (TBA)₂[Mo₆O₁₉] and (TBA)₄[Mo₈O₂₆] were synthesized according to the literature method.^{1,2} Other chemicals and reagents for synthesis were purchased from commercial sources and used without further purification.

Characterization

Single-crystal X-ray diffraction (SCXRD) measurements for **Ag₁₀-Mo₆** and **Ag₁₈-Mo₆** were performed on a Rigaku XtaLAB Pro diffractometer with Cu-K α radiation ($\lambda = 1.5418 \text{ \AA}$) at 200 K. Data collection and reduction were performed using the program CrysAlisPro.³ The two structures were solved with direct methods (SHELXS-2015)⁴ and refined by full-matrix least-squares on F2 using OLEX2,⁵ which utilized the SHELXL-2015 module.⁶ All non-hydrogen atoms were refined anisotropically and the hydrogen atoms were included in idealized positions. Notably, uncoordinated solvent molecules of **Ag₁₈-Mo₆** were a highly disordered result in the failure of identification. Therefore, the residual electron density was flattened out used the solvent mask protocol inside Olex2. The crystallographic data and selected bond distances were listed in Supplementary Table S1 and S2. The Powder X-ray diffraction (PXRD) patterns of **Ag₁₀-Mo₆** and **Ag₁₈-Mo₆** were collected on a Rigaku MiniFlex 600 diffractometer at 30 kV, and Cu-K α ($\lambda = 1.5418 \text{ \AA}$) at ambient temperature. The FT-IR spectra were recorded from KBr pellets in the range from 4000 to 400 cm⁻¹ on a Nicolet NEXUS 470-FTIR spectrometer. Thermogravimetry (TG) analyses were performed on a TGA Q500 apparatus from room temperature to 500 °C at a heating rate of 10 °C/min under nitrogen atmosphere. UV-visible diffuse-reflectance spectra were recorded with a UH4150 spectrophotometer. The photoluminescence emission spectra were carried out using a Horiba FluoroLog-3 fluorescence spectrometer. Photoluminescent decay of **Ag₁₀-Mo₆** was measured on the Horiba Fluorolog-3 spectrofluorometer equipped with a 355 nm-laser with a resolution time of 340 μ s at the room temperature. The photoluminescent quantum efficiency in powder form was measured using an integrating sphere on a HORIBA Fluorolog-3 spectrofluorometer. Elemental Analysis (EA) were carried out at on a FLASH EA 112 elemental analyzer.

Cyclic voltammogram (CV) of **Ag₁₀-Mo₆** and **Ag₁₈-Mo₆** were studied by CHI 660E electrochemical analyzer (CH Instruments Inc.) with a typical three-electrode cell consisting of graphite rod as a counter electrode, a silver/silver chloride (Ag/AgCl) as reference electrode, and a glassy carbon electrode (GCE) coated with the as-prepared catalysts ink as the working electrode. GCE was cleaned by sonication in dilute nitric acid solution, water, and ethanol after polished using 0.05 μ m alumina power and then dried at room temperature. As-prepared catalyst ink was made by 2 mg sample of **Ag₁₀-Mo₆** and **Ag₁₈-Mo₆** dispersed in 20 μ L of 5% Nafion, 50 μ L isopropanol, and 100 μ L water solution accompanied with ultrasound about 30 min, respectively. After a while, 4 μ L of the as-prepared catalyst ink will be loaded on the GCE and dried naturally.

Synthesis of [Ag₁₀(S^tBu)₆(CH₃CN)₈(Mo₆O₁₉)₂·2CH₃CN]_n (Ag₁₀-Mo₆**) and [Ag₁₈(S^tBu)₁₂(CH₃CN)₅(Mo₆O₁₉)₂·Mo₆O₁₉·2CH₃CN]_n (**Ag₁₈-Mo₆**)**

AgS^tBu (20 mg, 0.11 mmol) was dissolved in acetonitrile (4 mL) under vigorous stirring. Then CF₃SO₃Ag (25.6 mg, 0.10 mmol) and CF₃SO₃H (10 μ L) were added to the above solution. The resultant colorless and clear solution was further added by 1 mL CH₃CN solution containing (TBA)₄[Mo₈O₂₆] (10 mg, 0.0046 mmol) or (TBA)₂[Mo₆O₁₉] (10 mg, 0.007 mmol). Subsequently, when added (TBA)₄[Mo₈O₂₆], the clear solution was got. While the unclear solution was obtained after added (TBA)₂[Mo₆O₁₉] and filtrated after unremitting stirred for 5 min. The mixtures were evaporated slowly in the air at room temperature and allowed to stand in the dark for 3–5 days to give colorless needle-like and yellow flower-like crystals, respectively. The crystals formed were filtered off, washed with acetonitrile. Yield: 35% of **Ag₁₀-Mo₆**, 42% of **Ag₁₈-Mo₆** (based on Ag).

Elemental Analysis: **Ag₁₀-Mo₆** (C₄₄H₈₄Ag₁₀Mo₁₂N₁₀O₃₈S₆): calc. (%) C 13.97, N 3.70, H 2.23, S 5.08; found

C 13.78, N 3.75, H 2.12, S 4.97. **Ag₁₈-Mo₆** (C₆₂H₁₂₉Ag₁₈Mo₁₈N₇O₅₇S₁₂): calc. (%) C 12.54, N 1.65, H 2.19, S 6.48;
found C 12.41, N 1.49, H 2.12, S 6.36.

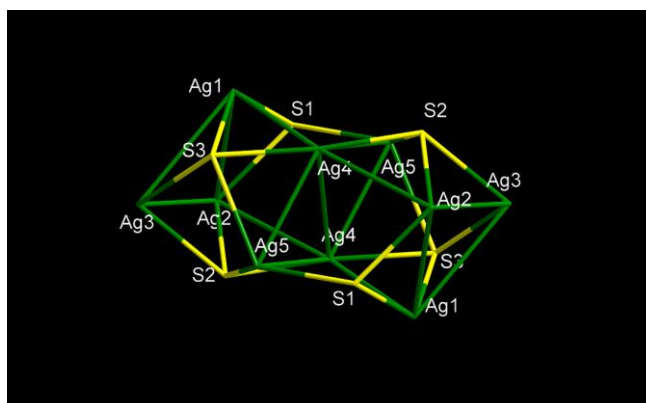


Fig. S1. Perspective view of Ag₁₀ cluster in **Ag₁₀-Mo₆**.

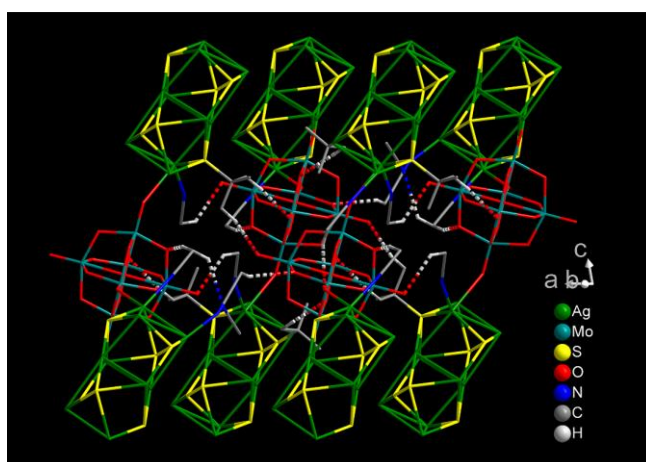


Fig. S2. The weak C–H···O weak interactions among adjacent chains in **Ag₁₀-Mo₆** with the H···O distances (C–H···O angles) are 2.579 Å (164.55°); 2.648 Å (136.53°); 2.464 Å (158.35°); 2.543 Å (131.78°); 2.500 Å (132.92°); 2.634 Å (164.56°); 2.594 Å (156.18°), respectively. The C–H···N weak interactions among adjacent chains, the C–H···N distance (C–H···N angles) is 2.630 Å (131.926°).

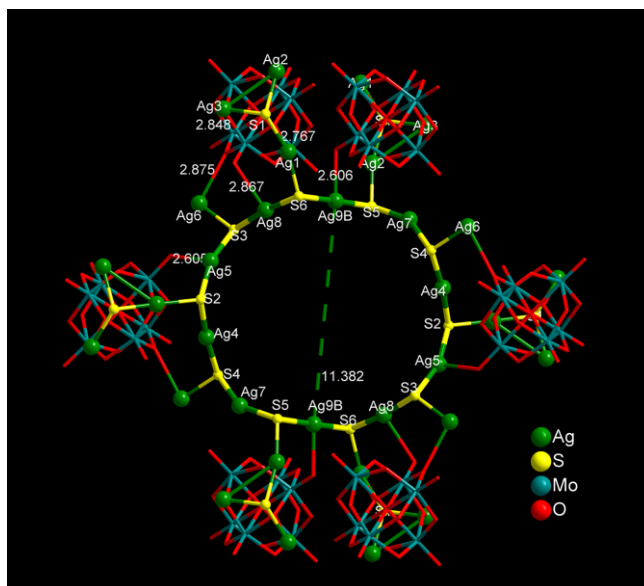


Fig. S3. $\text{Ag}_{18}\text{-Mo}_6$ contains 20-membered cycle- $\text{Ag}_{10}\text{S}_{10}$ constructed by alternating silver and sulfur atoms with a diameter of approximately 11.382 Å. Moreover, $[\text{Mo}_6\text{O}_{19}]^{2-}$ improves the stability of Ag–S plane by Ag–O bonds. CH_3CN , $-\text{tBu}$, and H atoms are omitted for clarity. Ag8–O14, 2.867 Å; Ag9–O18, 2.608 Å; Ag5–O17, 2.605 Å and Ag1–O2, 2.767 Å; Ag3–O6, 2.848 Å; Ag6–O11, 2.875 Å.

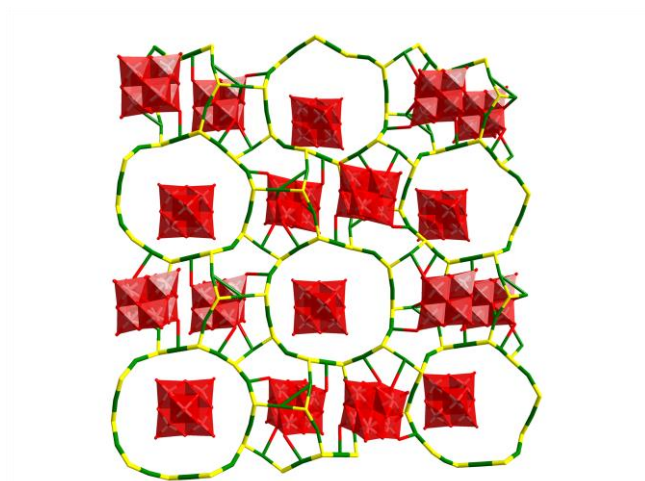


Fig. S4. Stacking structures of $\text{Ag}_{18}\text{-Mo}_6$. $[\text{Mo}_6\text{O}_{19}]^{2-}$ not only acts as counterions filled in the large gaps of cycle- $\text{Ag}_{10}\text{S}_{10}$ but also strengthens the structural stability by Ag–O bonds. Color code: Ag, green; S, yellow; N, blue; C, gray; Mo, teal; O, red. H atoms are omitted for clarity.

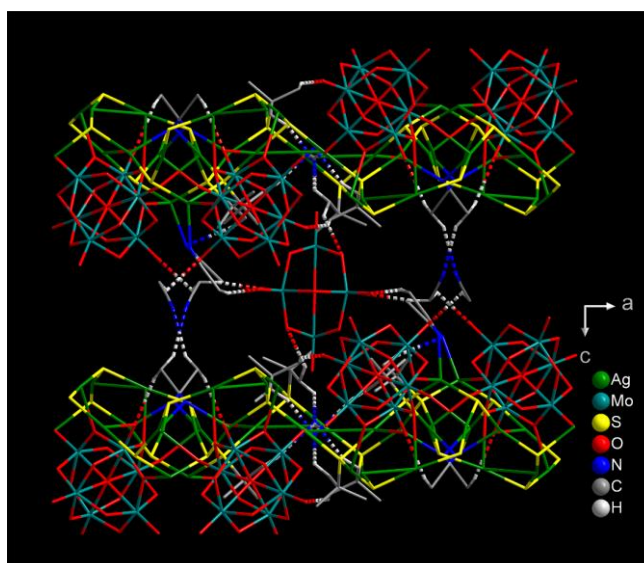


Fig. S5. The weak C–H···O weak interactions among adjacent sheets in **Ag₁₈-Mo₆** with the H···O distances (C–H···O angles) are 2.590 Å (144.77°); 2.320 Å (154.25°); 2.624 Å (143.36°); 2.433 Å (160.75°); 2.618 Å (112.69°); 2.318 Å (169.56°); respectively. The C–H···N weak interactions among adjacent sheets, the C–H···N distances (C–H···N angles) are 2.641 Å (154.06°); 2.671 Å (134.65°); 2.592 Å (158.30°); 2.277 Å (158.36°), respectively

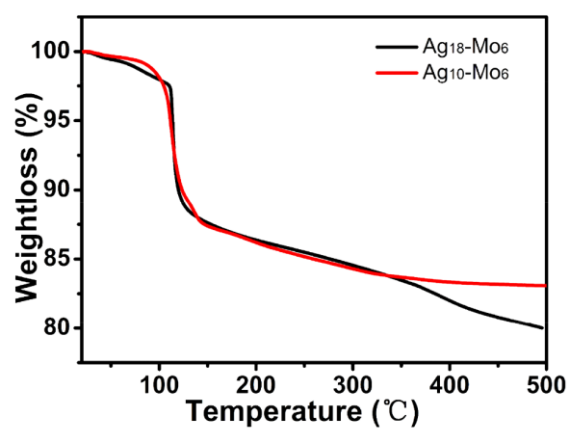


Fig. S6. TG analysis curves of **Ag₁₀-Mo₆** and **Ag₁₈-Mo₆** revealed that the mass loss beginning at about 90 °C is associated with the decomposition of the host framework.

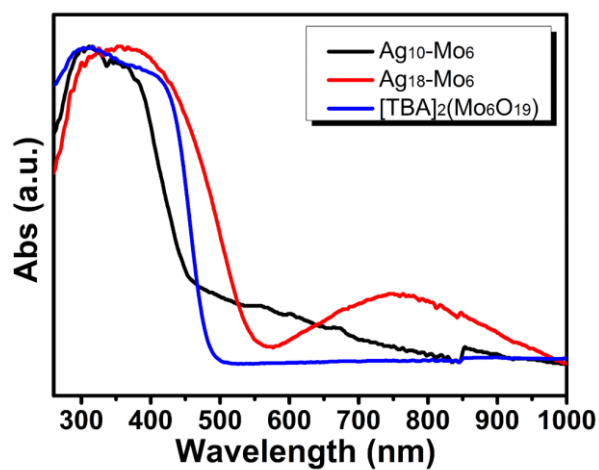


Fig. S7. UV-Vis diffuse-reflectance spectra of $\text{Ag}_{10}\text{-Mo}_6$, $\text{Ag}_{18}\text{-Mo}_6$ and $(\text{TBA})_2[\text{Mo}_6\text{O}_{19}]$ in solid states at room temperature.

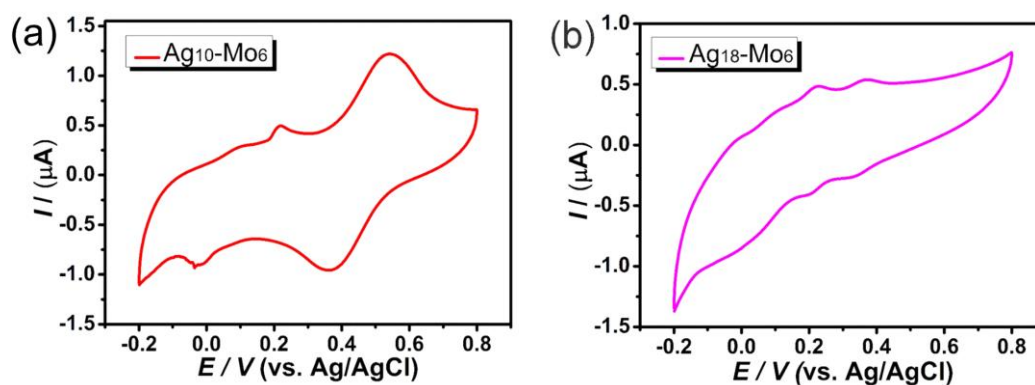


Fig. S8. Cyclic voltammogram of $\text{Ag}_{10}\text{-Mo}_6$ (a) and $\text{Ag}_{18}\text{-Mo}_6$ (b) in 0.5 M H_2SO_4 aqueous solution at the scanning speed of 50 mV/s.

Table S1. Crystal data and structure refinements for **Ag₁₀-Mo₆** and **Ag₁₈-Mo₆**.

| | Ag₁₀-Mo₆ | Ag₁₈-Mo₆ |
|---|--|---|
| CCDC number | 1950498 | 1950501 |
| Empirical formula | C ₄₄ H ₈₄ Ag ₁₀ Mo ₁₂ N ₁₀ O ₃₈ S ₆ | C ₆₂ H ₁₂₉ Ag ₁₈ Mo ₁₈ N ₇ O ₅₇ S ₁₂ |
| Formula weight | 3783.55 | 5938.01 |
| Temperature / K | 200.01(10) | 200.01(10) |
| Crystal system | Triclinic | orthorhombic |
| Space group | <i>P</i> $\bar{1}$ | <i>Pbcn</i> |
| <i>a</i> (Å) | 11.30672(10) | 27.3167(2) |
| <i>b</i> (Å) | 15.29988(14) | 19.80926(14) |
| <i>c</i> (Å) | 15.58799(14) | 27.71777(16) |
| α (°) | 63.3059(9) | 90 |
| β (°) | 87.7117(7) | 90 |
| γ (°) | 83.0788(7) | 90 |
| Volume (Å ³) | 2391.32(4) | 14998.72(18) |
| Z | 1 | 4 |
| ρ_{calc} g/cm ³ | 2.627 | 2.630 |
| μ /mm ⁻¹ | 30.289 | 32.382 |
| F(000) | 1792.0 | 11200.0 |
| Crystal size/mm ³ | 0.1 × 0.02 × 0.02 | 0.1×0.1×0.1 |
| Radiation | CuK α (λ = 1.54184) | CuK α (λ = 1.54184) |
| 2 Θ range for data collection/° | 6.348 to 146.692 | 5.51 to 145.186 |
| Index ranges | -13 ≤ <i>h</i> ≤ 14, -18 ≤ <i>k</i> ≤ 13, -19 ≤ <i>l</i> ≤ 19 | -23 ≤ <i>h</i> ≤ 33, -23 ≤ <i>k</i> ≤ 24, -34 ≤ <i>l</i> ≤ 27 |
| Reflections collected | 26058 | 56711 |
| Independent reflections | 9331 [<i>R</i> _{int} = 0.0411, <i>R</i> _{sigma} = 0.0385] | 14604 [<i>R</i> _{int} = 0.0429, <i>R</i> _{sigma} = 0.0343] |
| Data/restraints/parameters | 9331/6/555 | 14604/80/859 |
| Goodness-of-fit on F ² | 1.079 | 1.101 |
| Final R indexes [<i>I</i> ≥ 2 σ (<i>I</i>)] | <i>R</i> ₁ = 0.0443, <i>wR</i> ₂ = 0.1126 | <i>R</i> ₁ = 0.0515, <i>wR</i> ₂ = 0.1273 |
| Final R indexes [all data] | <i>R</i> ₁ = 0.0461, <i>wR</i> ₂ = 0.1145 | <i>R</i> ₁ = 0.0545, <i>wR</i> ₂ = 0.1289 |
| Largest diff. peak/hole / e Å ⁻³ | 1.08/-3.20 | 3.40/-2.10 |

$$R_1 = \frac{\sum ||F_o| - |F_c||}{\sum |F_o|}, wR_2 = \left[\frac{\sum w(F_o^2 - F_c^2)^2}{\sum w(F_o^2)^2} \right]^{1/2}$$

Table S2. Selected bond distances (Å) for **Ag₁₀-Mo₆** and **Ag₁₈-Mo₆**.

| Ag₁₀-Mo₆ | | | |
|---------------------------------------|------------|----------------------|------------|
| Ag1–Ag2 | 3.3044(6) | Ag3–S2 | 2.6607(12) |
| Ag1–Ag4 ¹ | 2.9723(5) | Ag3–S3 ¹ | 2.4745(11) |
| Ag1–S1 | 2.4494(14) | Ag3–N3 | 2.136(5) |
| Ag1–S3 ¹ | 2.4969(12) | Ag4–Ag1 ¹ | 2.9724(5) |
| Ag1–O1 | 2.815(4) | Ag4–Ag4 ¹ | 3.3612(7) |
| Ag1–N1 | 2.258(6) | Ag4–Ag5 | 3.0253(5) |
| Ag2–Ag3 | 3.2134(6) | Ag4–Ag5 ¹ | 3.1530(6) |
| Ag2–Ag4 | 3.3648(6) | Ag4–S2 | 2.3718(12) |
| Ag2–S1 | 2.4431(13) | Ag4–S3 | 2.3991(12) |
| Ag2–S2 | 2.5583(12) | Ag5–Ag4 ¹ | 3.1530(6) |
| Ag2–N2 | 2.205(5) | Ag5–S1 | 2.4753(12) |
| Ag₁₈-Mo₆ | | | |
| Ag1–S1 | 2.397(2) | Ag7–S4 | 2.409(2) |
| Ag1–S6 ¹ | 2.388(2) | Ag7–S5 | 2.409(2) |
| Ag2–Ag3 | 3.3206(11) | Ag7–N1 | 2.632(11) |
| Ag2–S1 | 2.367(2) | Ag8–S3 | 2.373(2) |
| Ag2–S5 | 2.365(2) | Ag8–S6 | 2.375(2) |
| Ag3–S1 | 2.381(2) | S4–Ag4 ² | 2.371(2) |
| Ag3–S2 | 2.378(2) | S5–Ag9B ³ | 2.339(3) |
| Ag4–S2 | 2.377(2) | S5–Ag9A ³ | 2.515(6) |
| Ag4–S4 ¹ | 2.371(2) | S6–Ag1 ² | 2.388(2) |
| Ag5–S2 | 2.404(2) | S6–Ag9B | 2.381(3) |
| Ag5–S3 | 2.399(2) | S6–Ag9A | 2.405(4) |
| Ag6–S3 | 2.462(2) | Ag9B–S5 ⁴ | 2.339(3) |
| Ag6–S4 | 2.458(2) | Ag9B–N2 | 3.21(4) |
| Ag6–N4A | 2.394(14) | Ag9A–S5 ⁴ | 2.515(6) |
| Ag6–N4B | 2.281(14) | | |

Ag₁₀-Mo₆: ¹1 – x, 2 – y, 1 – z; **Ag₁₈-Mo₆:** ¹1/2 + x, 3/2 – y, – z; ²3/2 – x, – 1/2 + y, + z; ³3/2 – x, 1/2 + y, + z; ⁴– 1/2 + x, 3/2 – y, – z.

Reference

1. R.-W. Huang, Q.-Q. Xu, H.-L. Lu, X.-K. Guo, S.-Q. Zang, G.-G. Gao, M.-S. Tang and T. C. W. Mak, *Nanoscale*, 2015, **7**, 7151-7154.
2. S. Ikegami, A. Yagasaki, *Mater.*, 2009, **2**, 869-875.
3. CryaAlisPro 2012, Aligent Technologies. Version 1.171.36.31.
4. G. M. Sheldrick, *Acta Crystallogr. Sect. A*, 2015, **71**, 3-8.
5. O. V. Dolomanov, L. J. Bourhis, R. J. Gildea, J. A. K. Howard, H. Puschmann, *J. Appl. Cryst.*, 2009, **42**, 339-341.
6. G. M. Sheldrick, Crystal structure refinement with SHELXL. *Acta Cryst. C*, 2015, **71**, 3-8.